Space Suit Thermal Dynamics

Anthony B. Campbell, Ph.D. Candidate
Satish S. Nair, Ph.D., P.E., Member ASHRAE
and John B. Miles, Ph.D., P.E.
University of Missouri - Columbia

John V. Iovine
Lockheed Martin Space Missions Systems & Sciences Co.

Chin H. Lin, Ph.D.
NASA Johnson Space Center

ABSTRACT

The present NASA space suit (the Shuttle EMU) is a self-contained environmental control system, providing life support, environmental protection, earth-like mobility, and communications. This study considers the thermal dynamics of the space suit as they relate to astronaut thermal comfort control. A detailed dynamic lumped capacitance thermal model of the present space suit is used to analyze the thermal dynamics of the suit with observations verified using experimental and flight data. Prior to using the model to define performance characteristics and limitations for the space suit, the model is first evaluated and improved. This evaluation includes determining the effect of various model parameters on model performance and quantifying various temperature prediction errors in terms of heat transfer and heat storage. The observations from this study are being utilized in two future design efforts, automatic thermal comfort control design for the present space suit and design of future space suit systems for Space Station, Lunar, and Martian missions.

1.0 INTRODUCTION

Extravehicular activity (EVA) is any activity performed by an astronaut, in the extravehicular mobility unit (EMU), when outside the controlled environment of the spacecraft or space station. The EMU or space suit is self-contained, providing life support, environmental protection, earth-like mobility, and communications (Figure 1). The Apollo EMU was the predecessor of the Shuttle EMU and was designed for less frequent and shorter EVAs. The next

generation space suit is being designed to handle the increased EVA demands for construction and maintenance of the Space Station as well as planned Lunar or Martian missions.

The current Shuttle EMU system diagram and the associated heat loads are given in Figure 2. The PLSS interacts with the suit via two loops; the water-cooling loop (WCL) which passes through the liquid cooling garment (LCG) and the ventilating loop (VL) which passes through the ventilation garment (VG). The thermal state of the EMU is affected primarily by the environmental heat load, by the astronaut's metabolic heat load, and by the temperature control valve (TCV) position chosen by the astronaut.

The WCL typically picks up 60-80% [Cam98] of the astronaut's metabolic heat load in the suit via the LCG and rejects that heat to space through sublimation of feedwater in the sublimator. The temperature of the water entering the LCG is controlled by the temperature control valve (TCV) position which the astronaut selects. The TCV is a proportional valve which diverts part of the circulating water to the sublimator to provide appropriate cooling. This is a cooling device only; no active heating is provided in the WCL or VL. Therefore the only heat source in the system is the metabolic heat produced by the astronaut. The VL typically picks up 20-40% [Cam98] of the astronaut's metabolic heat load through sensible and latent heat transfer in the VG and rejects it in the sublimator. Additional requirements on the VL are the need to remove carbon dioxide, remove sweat and exhaled moisture, and replace the oxygen consumed.

The Shuttle EMU is designed to accommodate the following EVA mission [Ham92]: (i) total duration of 7 hours maximum, consisting of 15 minutes for egress, 6 hours for useful EVA tasks, 15 minutes for ingress and a 30 minute reserve; (ii) an average metabolic rate of 1000 Btu/hr (293 W) for 7 hours; (iii) peak metabolic rates of 1600 Btu/hr (469 W) for 15 minutes at any time within the 7 hour EVA; and (iv) minimum rate of 400 Btu/hr (117 W) for 30 minutes after an average work rate of 1000 Btu/hr (293 W) and followed by a rate of 700 Btu/hr (205 W) for up to 30 minutes. The EMU consists of two main subcomponents, the space suit assembly (SSA) and the portable life support system (PLSS). While Figure 2 shows schematically how the

WCL and VL are arranged, Figures 1a and 1b show clearly that the physical system is much more complex. A primary structure in the PLSS is a stainless steel valve module, with all of the major components shown in Figure 2 being connected to it. The majority of the piping and ducting segments of the PLSS are contained in the valve module.

The objective of this paper is two-fold. The first is to provide an overview of the thermal dynamics of the Shuttle EMU and define performance characteristics and limitations for the system. The second is to evaluate and improve the current NASA Shuttle EMU thermal model (SINDA EMU) and quantify the effect of various EMU model parameters on thermal behavior of the EMU model. The limitations and the observations from this study can be utilized in two future design efforts, automatic thermal control design for the present Shuttle EMU and design of future EMU systems for Space Station, Lunar, and Martian missions. Specifically, the paper: (i) describes the thermal dynamics issues for the Shuttle EMU, (ii) quantifies model prediction errors in terms of heat transfer and heat content errors and defines the limitations of the Shuttle EMU model, (iii) analyzes some of the basic modeling assumptions and determines enhancements to the Shuttle EMU model, (iv) performs simulations using three metabolic rates and three environments (both spanning typical ranges) to determine the associated environmental heat leaks and to check whether thermal comfort is maintained, (v) studies four EMU variables representative of the overall thermal state of the human-EMU system in terms of their operating ranges and response times, and defines the performance envelope for the EMU in terms of metabolic rate and environment.

2.0 SINDA EMU MODEL

The original NASA JSC Shuttle EMU or SINDA EMU computer model was developed for detailed transient thermal simulation of the Space Shuttle EMU [Lin78]. The model accounts for conductive, convective, and radiative heat transfer between the EMU and crewperson, between the EMU and environment, and within the PLSS. The thermoregulatory system of the crewperson is modeled using the 41-Node Man program [Bue89]. The 41-Node Man models the human body as 10 sets of concentric cylinders representing the core, muscle, fat, and skin

3

[Smi93,Fre97]. The SINDA EMU model was created using the Systems Improved Numerical Differencing Analyzer (SINDA) which is a general analyzer for nodal thermal networks.

Using the lumped parameter representation of the EMU, the heat balance equation for node i in the network is given by

$$C_i \frac{dT_i}{dt} = \sum_j G_{ij} \left(T_j - T_i \right) + Q_i$$

where C_i is the heat capacitance of the node, G_{ij} is the conductance (conductive, convective, radiative, or flow) between node i and adjacent nodes j, and Q_i is the heat source term for node i. The SINDA network for the entire EMU consists of 490 nodes and 1134 conductors. The SSA, EVVA, and DCM thermal networks consist of 255, 58, and 27 nodes, respectively. The PLSS network comprises 9 TMG nodes, 9 hard cover nodes, 42 internal structure nodes, 33 fluid nodes, 23 tube nodes, and 5 sublimator nodes. The environmental temperatures are represented by 4 nodes.

2.1 Experimental Validation - A series of fully suited vacuum experiments were run in the Crew and Thermal Systems Division's 11 foot chamber at Johnson Space Center (JSC) [Tho94]. Data from the three complete experiments, where the subjects completed 5.5 hours of exercise attempting to replicate the desired metabolic profile, is used in this study [IL96,Cam97].

The recorded metabolic rate and TCV positions from the suited vacuum experiments were input to the SINDA EMU model to replicate the experiments. The experimentally recorded metabolic rate and TCV positions for Subject 1 are shown in Figure 3. The first stage of validation uses the integrated SINDA EMU model which includes the human, suit, and PLSS, for generating predictions. The second stage looks at the PLSS submodel free from the effects of the human and suit thermal models. The third stage looks at the human-suit submodel free from the effects of the PLSS thermal model.

Integrated Model Analysis - The integrated model analysis uses the complete SINDA EMU model which includes the human, suit, and PLSS submodels. The range of temperature differences between the integrated model predictions and experimental data for the 3 subjects can be seen in Table 1.

The simulated and experimental LCG water inlet temperatures (Tin,lcg) for Subject 1 are shown in Figure 4. The model has trouble predicting the transients after a TCV change, with the simulated temperature changing faster than the experimental data. The other problem that can be observed from Figure 4 is that the simulated inlet LCG temperature is 4 to 5°F (2.2 to 2.8°C) lower than experimental data during the high metabolic rate period from approximately 4.5 hours to 5.1 hours. The simulated VG gas inlet and outlet temperatures for Subject 1 showed errors of 0 to -3°F (0 to -1.7°C) and 1 to 6°F (0.6 to 3.3°C), respectively, when compared with experimental data. The simulated VG gas inlet and outlet dew points for Subject 1 showed errors of -3 to +4°F (-1.7 to 2.2°C) and +3 to +6°F (1.7 to 3.3°C), respectively, when compared with experimental data. The body core temperature errors are up to ±2°F (1.1°C), which is very large considering that the actual body core temperature only fluctuates by ±1°F (0.6°C). The average skin temperature also shows a large difference between simulation and experimental data. For the valve module temperatures, some differences between the experimental and simulated temperatures were expected, approximately 3°F (1.7°C), due to the experimental temperatures being measured at single points and the simulated temperatures representing lumped or averaged temperatures. The difference of approximately 18°F (10°C) between the simulated HUT interface valve module temperature and the experimental data would therefore seem to indicate that there are modeling problems.

PLSS Submodel Analysis - In the PLSS submodel analysis, the LCG and VG outlet (PLSS inlet) conditions were prescribed from experimental data and the LCG and VG inlet (PLSS outlet) predictions were compared to experimental data (Table 2).

As shown in Figure 5, the open loop PLSS submodel does a better job of tracking the experimental temperatures and of predicting the transients associated with a TCV change compared to the integrated model. The simulation prediction is still 1 to 2°F (0.6 to 1.1°C) lower than the experimental data for the high metabolic rate period from approximately 4.5 hours to 5.1 hours. The VG gas inlet temperature and dew point tracks the experimental temperature with an offset of -4 to +1°F (-2.2 to +0.6°C) and -4 to +5°F (-2.2 to +2.8°C), respectively. Neither the

5

VG gas inlet temperature nor the dew point show dramatic improvement over the integrated model predictions.

Suit Submodel Analysis - In the suit submodel analysis, the LCG and VG inlet (PLSS outlet) conditions were prescribed from experimental data and the LCG and VG outlet (PLSS inlet) predictions were compared to experimental data.

The simulation and experimental LCG water outlet temperatures for Subject 1 are shown in Figure 6. Similar to the PLSS analysis, this submodel tracks the experimental temperature better than the integrated model. One problem that can be observed is that the simulation is approximately 1°F (0.6°C) higher than the experimental data. The VG outlet temperature tracks the experimental temperature with an offset of approximately +7°F (3.9°C). The VG outlet dew point does not track the experimental temperature well with the simulated dew point being rather erratic and differing from the experimental data by -7 to +8°F (-3.9 to +4.4°C). The predicted body core temperature showed worse agreement with experimental data than the integrated model simulation with the maximum error being -2°F (1.1°C). The predicted average skin temperature comparison showed similar trends as the integrated model simulation differing from experimental data by 5 to 9°F (2.8 to 5°C).

Validation Conclusions - Simulations have shown that an open loop error of 1°F (0.6°C) in the WCL translates to closed loop errors of 2.5 to 20°F (1.4 to 11.1°C) depending on TCV position, metabolic rate, and location of error. Therefore, a comparison of the differences between simulation and experimental data for the closed loop integrated SINDA EMU model and the open loop PLSS and suit analyses should be done carefully.

The simulated LCG inlet water temperature responds much faster to a TCV change than the experimental data. Comparing the predicted temperatures in the integrated and PLSS analyses showed that the WCL transient problems are due to neglecting fluid transport delays in the WCL. During high TCV portions, the simulated LCG inlet water temperature was colder than experimental data. This could indicate a problem with the curve which defines the WCL

flow through the sublimator as a function of TCV, an error in recording TCV position, or a weakness in the sublimator model.

The 41-Node Man model's weaknesses were apparent from the predicted body core and average skin temperatures in the suit submodel analysis. The LCG and VG outlet temperatures being too high for the majority of the simulation are due to the high skin temperature increasing the heat transfer between the skin and the LCG. The VG outlet dew point error in the suit submodel analysis does not improve dramatically over the integrated SINDA EMU model which would therefore indicate that the problems with the dew point are primarily due to the human and suit models. The VG outlet dew point errors are probably due to the 41-Node Man model's sweat prediction along with the complexity of modeling the evaporation and condensation from skin covered by a TCU and LCG.

The large errors in the valve module temperature demonstrated problems in the PLSS heat balance. The focus on improving the model in the past has been on WCL, VL, and body temperatures, which resulted in some EMU variables not being predicted accurately. The valve module temperature errors could translate to WCL and VL temperature errors since both loops interact with the valve module.

2.2 Quantifying Errors - The model errors revealed in the previous section are now discussed and quantified in terms of the heat transfer or heat content which the errors represent. To quantify errors in heat transfer rates associated with WCL and VL temperature errors, consider

$$\dot{Q}_{error} = \dot{m}c_p(T_{predicted} - T_{actual})$$

where $\dot{m}$ is the mass flow rate and c_p is the specific heat of the fluid. For the WCL, with a flow rate of 240 lbm/hr, $\dot{m}c_p = 240$ $BTU/hr-°F$. For the VL, assuming pure oxygen flowing at 6 lbm/hr with a pressure of 4.3 psi and a temperature of 80°F, $\dot{m}c_p = 1.88$ $BTU/hr-°F$. A 1° (0.6°C) error between the predicted and actual WCL and VL temperatures would therefore translate to an error in the heat balance of the model of 240 BTU/hr (70 W) and 2 BTU/hr (0.6 W), respectively.

The heat transfer associated with a VL dew point error of $\pm 5°F$ ($2.8°C$) can be calculated as

$$\dot{Q}_{error} = \dot{m}_{gas}\left(h_{45°F} - h_{40°F}\right) = 35.8 \ BTU/hr \ (10.5 \ W)$$

where $\dot{m}_{gas}$ is the mass flow rate of the gas in the VL, $h_{45°F}$ and $h_{40°F}$ are the enthalpy of the moist air at dew points of 45 ($7.2°C$) and $40°F$ ($4.4°C$) respectively, and the dry bulb temperature of the gas is assumed to be $70°F$ ($21°C$). As the dew point temperature increases, the $\pm 5°F$ ($2.8°C$) dew point error would represent a larger heat transfer error (e.g. 46 BTU/hr (13.5 W) for dew points of 45 ($7.2°C$) and $50°F$ ($10°C$) with a dry bulb temperature of $70°F$ ($21°C$)). Therefore the VL temperatures and dew points are much harder to predict accurately than the WCL temperatures since they are more sensitive to heat load and heat transfer errors. While not as significant in the overall EMU heat balance, the VL temperatures and dew points do still need to be predicted accurately since they are important in determining the astronaut's thermal comfort [Cam98].

The accuracy for the WCL and VL predictions and a comparison of the associated heat transfer for the average metabolic rate during Shuttle EVAs (751 BTU/hr, 220 W) are given in Table 3a. This analysis shows that the WCL temperature errors are more significant than the VL temperature or dew point errors. The heat transfer associated with the WCL temperature is 32% of the average metabolic rate and therefore improving the WCL temperature accuracy should be a higher priority.

The temperature prediction errors for the valve module, skin, and core temperatures must be quantified in terms of the heat content error. The heat content error is calculated by

$$Q_{error} = mc_p(T_{predicted} - T_{actual})$$

where m is the mass represented by the specific temperature being discussed. The valve module has a mass of 17 lbm (7.7 kg), and its mass specific heat product is $mc_p=2.04$ BTU/°F (1.1 W-hr/°C). The heat content error for a valve module temperature prediction error of $18°F$ ($10°C$) is therefore 36.72 BTU (10.8 W-hr). The mass specific heat product for the skin of an average man is $mc_p=7.07$ BTU/°F (3.7 W-hr/°C). The heat content error for an average skin temperature

8

prediction error of 5°F (2.8°C) is therefore 35.35 BTU (10.4 W-hr). The mass specific heat product for the core segment skeleton and viscera of an average man is mc_p=42.92 BTU/°F (22.6 W-hr/°C). The heat content error for core temperature prediction error of 1°F (0.56°C) is therefore 42.92 BTU (12.6 W-hr).

The accuracy for the valve module, skin, and core temperatures and a comparison of the associated heat content error to the ± 65 BTU (19 W-hr) comfort band (Figure 12) are given in Table 3b. The heat content errors for all three temperatures are over 50% of the ± 65 BTU (19 W-hr) comfort band. Therefore it is difficult to confidently predict thermal comfort with the current SINDA EMU model due to these temperature prediction errors.

3.0 MODEL ENHANCEMENTS

Some of the basic assumptions made in modeling the Shuttle EMU are addressed in this section and model enhancements investigated. The assumptions investigated are: (i) neglecting thermal masses, (ii) neglecting transport delays, (iii) the LCG model, and (iv) the valve module model.

3.1 Negligible Thermal Mass - The two masses considered are the mass of water in the WCL, approximately 1 lbm. (0.45 kg), and the mass of gas in the VL, approximately 0.0004 lbm (0.00018 kg). The valve module and feedwater storage tanks are the significant masses in the EMU system weighing approximately 17 lbm (7.7 kg) and 37 lbm (16.8 kg), respectively, and are included in SINDA EMU. The mass of the gas in the VL and water in the WCL are 0.002% and 6% of the mass of the valve module which is the major structure with which the VL and WCL interacts. Simulations showed that the mass of the water in the WCL and of the gas in the VL can be neglected for transient and steady state predictions.

3.2 Transport Delays - WCL and VL transport delays are not accounted for in the SINDA EMU lumped parameter representation of the PLSS. The VL transport delays are relatively short and can be neglected [Cam97], but the WCL transport delays are more significant. The total transport delay for a particle of water (Figure 8) to pass through the LCG, through the heat exchanger, and back to the LCG ranges from 11 seconds for a TCV position of

9

11 (maximum cooling) to 240 seconds for a TCV position of 0 (minimum cooling) [Cam96]. Therefore if the WCL transport delays are ignored, the model predictions can be off by as much as 4 minutes for the full hot TCV setting. The higher the TCV position or the more cooling that is desired, the less the transport delay errors in the model.

Several simplified models (as in Figure 8) of the WCL were implemented to determine the effect of the various transport delays on the WCL temperature response. It was found that the addition of the pipe transport delays by themselves makes only a minor difference in the response of the LCG inlet water temperature. The addition of the LCG transport delay only, significantly decreases the errors in the transient responses and indicates that the majority of the transient errors in the earlier plots are due to the LCG transport delay not being included.

The SINDA EMU model was modified so that different transport delays could be included for the LCG. The model was then run for the Subject 1 case and the inlet LCG temperature compared with experimental data in Figure 9. From this analysis, it was determined that a transport delay of 60 seconds showed the best agreement between the simulation and experimental transients. In reality, the LCG transport delay should not be this large, but since the delays throughout the PLSS were not modeled, the LCG transport delay is accounting for some of this delay. This modification of the LCG model to include the 60 second transport delay was a definite enhancement of the transient performance of the model.

3.3 LCG Model - The current LCG model calculates the overall heat transfer coefficient (UA) between the skin and LCG as

$$UA = 0.45 \cdot UA_o \left[1 - 1.08 \exp\left(-0.0166 \dot{m}_{lcg}\right) \right]$$

where $UA_o = 75.5 - 1.17 T_{in,lcg} + 0.0327 T_{in,lcg}^2 - 0.31 \times 10^{-3} T_{in,lcg}^3$, with $UA_o > 27.55$ for all $T_{in,lcg}$; $\dot{m}_{lcg}$ and $T_{in,lcg}$ are the flow rate and water inlet temperature of the LCG. The overall heat transfer to the LCG, using the effectiveness-NTU method, is

$$q_{lcg} = \dot{m}_{lcg} c_{p,l} \left(T_{out,lcg} - T_{in,lcg} \right) = \varepsilon \dot{m}_{lcg} c_{p,l} \left(T_{skin} - T_{in,lcg} \right)$$

where $\overline{T}_{skin}$ is the weighted average skin temperature of the trunk, arms, and legs. Assuming the heat capacitance of the skin is much larger than the heat capacitance of the LCG water, the effectiveness is defined as $\varepsilon = 1 - e^{-NTU}$, with $NTU = UA / \dot{m}_{lcg}c_{p,l}$

The outlet LCG temperature is calculated as

$$T_{out,lcg} = T_{in,lcg} + (1 - e^{-NTU})(\overline{T}_{skin} - T_{in,lcg})$$

For the LCG model, the basic assumption is that the only heat transfer with the LCG is between the skin and the LCG and therefore this model ignores any sensible or latent heat transfer with the gas in the suit. The condensation and evaporation of water on the LCG is modeled for the gas in the VG, but the heat transfer from these phenomena have no direct effect on the LCG outlet temperature. The heat transfer from the coolant of the LCG to each human body segment, $q_{lcg,i}$, is calculated as

$$q_{lcg,i} = f_i \dot{m}_{lcg}c_{p,l}(T_{out,lcg} - T_{in,lcg})$$

where f_i is the percent of flow of coolant in the LCG to each body segment.

The presence of the thermal comfort undergarment (TCU), a crew preference item, is modeled by the 0.45 factor in the current UA model to reflect increased resistance; it results in a significant drop in LCG heat transfer.

Experimental Validation - The coupling of the 41-Node Man model and the LCG UA model makes this model a complex one. The Suit Submodel Analysis showed that some of the errors in the WCL temperatures are due to the human-suit portion of the SINDA EMU model. To isolate whether these errors are due to the LCG model or the human thermal model, the LCG model was used with experimental data to determine the LCG outlet temperature as

$$T_{out,lcg} = \overline{T}_{skin} - (\overline{T}_{skin} - T_{in,lcg})\exp\left(-UA_{mod}/\dot{m}_{lcg}c_{p,l}\right)$$

where $T_{in,lcg}$ and T_{skin} are from the experimental data. UA_{mod} was calculated from the experimental $T_{in,lcg}$ and a constant $\dot{m}_{lcg}$ of 240 lbm/hr (109 kg/hr). This analysis is open loop in the sense that it disregards the effect of UA_{mod} on T_{skin} and $T_{in,lcg}$ and that it does not allow errors from previous time steps to effect the present temperature prediction. The calculated outlet LCG temperature agreed well with experiments, being generally within 0.5°F (0.28°C) of the data. The model calculated UA did not match well in the transient sense and had smaller

fluctuations than the experimental data (Figure 10). The model UA is of the same average value as the experimental data with the exception of the large peak in the experimental UA value around 2.5 hours corresponding to a 2°F (1.1°C) error seen in the LCG outlet temperature. From this analysis it can be concluded that LCG outlet temperature is not extremely sensitive to errors in the LCG UA model and that the primary source of errors in the LCG outlet temperature are the 41-Node Man's skin temperature prediction.

LCG UA Model Comparison - A revised LCG UA model was developed which calculates the UA value based upon the human latent heat load. The two formulations (function of LCG inlet temperature or function of latent heat load) of the LCG UA model are investigated using the same process as the previous section of calculating the LCG outlet temperature based on experimental data. For the LCG outlet temperature prediction, the UA model based on the LCG inlet water temperature performs much better than the UA model based on the human's latent heat load. The calculated LCG UAs for both formulation of the UA model can be seen with experimental data in Figure 10. The latent heat load based UA was generally lower than the inlet water temperature based UA and the experimental data. While the latent heat load model is more intuitive than the inlet water temperature based model, these calculations support the use of the inlet water temperature based UA model and demonstrate the sensitivity of the latent heat load based UA to errors in the sweat rate model.

LCG Flow Rate - Analysis of the experimental data showed that the flow rate for Subject 1 in the experiments was actually 261 lbm/hr while SINDA EMU assumes a constant 240 lbm/hr (109 kg/hr). Using the same method as the previous section, the LCG outlet temperature was calculated for constant flow rates of 240 and 261 lbm/hr (109 and 118 kg/hr). This analysis showed that the LCG flow rate has only a small effect, ± 0.1°F (0.056°C), on the LCG outlet water temperature and so the approximation of a constant 240 lbm/hr (109 kg/hr) is acceptable.

LCG Modeling Conclusions - Based on the cited analyses, the SINDA EMU errors in LCG outlet water temperature are primarily due to the errors in $T_{in,lcg}$ (errors from previous time steps) and T_{skin} (errors from 41-Node Man Model), and not the LCG UA model. Agreement

12

between calculated and experimental LCG outlet water temperatures does not mean that the LCG-Human interaction is modeled well at individual parts of the body, but does mean that the LCG UA model adequately describes the overall heat transfer between the human and the LCG. The focus of future LCG modeling should be on modeling the heat transfer between the LCG, skin, and gas for various parts of the body, therefore allowing a more detailed prediction of localized thermal comfort.

3.4 Valve Module - The valve module is the central structure of the PLSS through which the WCL and VL flow and to which the various PLSS components are connected. The conductance between the valve module and sublimator plate is a parameter which has been adjusted in the past to improve model agreement with experimental data. A value of 10 BTU/hr-°F (5.3 W/°C) was chosen as a best fit of the data. To determine the sensitivity of the model to this conductance value, SINDA EMU simulations were run with the conductance set at 0, 7.5, 10, and 12.5 BTU/hr-°F (0, 4.0, 5.3, and 6.6 W/°C).

The ± 25% variation from the nominal value corresponds to a ± 1°F (0.6°C) in the LCG inlet water temperature, a ± 0.5°F (0.3°C) variation in the VG inlet gas temperature, a ± 0.25°F (0.14°C) variation in the VG inlet dew point, and a ± 2.5°F (1.4°C) variation in the valve module temperature. Larger conductance values cause LCG inlet, VG inlet, and valve module temperatures to be lower. Therefore the higher the conductance between the cold sublimator plate and the valve module, the cooler the valve module. For higher sublimator flow rates (higher TCV positions), the difference between the temperature responses for the four cases is less than the difference for lower sublimator flow rates. When the TCV is set to a higher position, the valve module temperature is lower and therefore the temperature difference between the sublimator plate and the valve module is smaller. Therefore the sensitivity of the various temperature responses to errors in the conductance value are less for high TCV positions since the valve module temperature is closer to the sublimator temperature of 32°F (0°C). This analysis illustrates the significant effect that the valve module temperature has on the WCL and

VL temperatures and the importance of modeling the interactions between valve module and the various components.

4.0 PERFORMANCE CHARACTERISTICS AND SIZING ISSUES

The thermal performance characteristics of the Shuttle EMU are discussed in terms of the environmental limitations and the operating ranges and response times for various EMU thermal variables. The four primary EMU variables discussed in terms of their operating ranges and response times are the inlet LCG temperature, the inlet VG temperature, the inlet VG dew point, and the temperature of the valve module in the PLSS. These variables were chosen because they are representative of the overall thermal state of the human-EMU system and significantly affect thermal comfort.

4.1 Environment - The purpose of this section is to quantify the thermal environments and metabolic rate ranges the Space Shuttle EMU is able to accommodate while maintaining the astronaut's thermal comfort. To do this, a series of simulations were performed using the current SINDA EMU algorithm which chooses the proper sublimator flow rate based on the total body heat storage thermal comfort definition shown in Figure 12. Metabolic rates of 400, 751, and 1276 BTU/hr (117, 220, and 374 W) were prescribed along with three different environmental sink temperatures and the simulations run for two hours each. The metabolic rates of 400, 751, and 1276 BTU/hr are the statistical minimum, total, and maximum metabolic averages from Space Shuttle EVAs on STS-37 through STS-82 [TT97]. These 9 two-hour simulations were used to generate Tables 4 and 5.

Table 4 lists the orbital environments (equivalent radiative sink temperatures) for Space Shuttle EVAs and the associated heat leaks for the cold, neutral, and hot thermal environments. A general "rule of thumb" is that the suit heat leak and PLSS heat leak are 2/3 and 1/3 of the total heat leak from the environment to the EMU which ranges from approximately -449 to +815 BTU/hr (-132 to +239 W).

Table 5 shows the Shuttle EMU thermal comfort rating for the nine 2-hr EVA simulations. This table was generated by evaluating the difference between the total body heat

storage and nominal comfort line in Figure 12 and comparing it with the ± 65 BTU (± 19 W-hr) comfort band.

For the cold environment with a low metabolic rate, the EMU was able to provide thermal comfort for almost 45 minutes before the body heat storage passed out of the ± 65 BTU (± 19 W-hr) comfort band. For the hot thermal environment with a high metabolic rate, the EMU was able to provide thermal comfort for 13 minutes before the body heat storage passed out of the ± 65 BTU (± 19 W-hr) comfort band. Therefore, it can be concluded that the unmodified EMU can provide for the astronaut's thermal comfort for only short periods of time in cold environments with low metabolic rates and in hot environments with high metabolic rates.

Based on this analysis, for the astronaut to remain comfortable in the cold environment with a low metabolic rate, it is necessary to modify the EMU to include heating or to decrease the heat leak by increasing the TMG insulation. Considering at the high metabolic rate case, the EMU would need a greater cooling capacity or increased TMG insulation in order for it to be used in the neutral to hot environments for two or more hours at the high metabolic rate of 1276 BTU/hr (374 W). If a high metabolic rate in a neutral to hot thermal environment is anticipated, not wearing the TCU would double the LCG heat transfer coefficient (UA) and therefore allow the EMU to provide thermal comfort in this extreme condition for a two-hour EVA. The PLSS is capable of providing the necessary cooling for a high metabolic rate in a hot environment for short periods of time subject to the 10 lb. constraint on the amount of sublimator feedwater the PLSS can carry.

4.2 Operating Ranges - The operating ranges of the LCG inlet water temperature $(T_{in,w})$, VG inlet gas temperature $(T_{in,vg})$, VG inlet gas dew point $(T_{in,dewpt})$, and the PLSS valve module temperature at the HUT interface (T_{vm}), were determined with SINDA EMU by setting the metabolic rate to the average minimum of 400 BTU/hr (117 W) and maximum of 1276 BTU/hr (374 W) for Shuttle EVAs and using the minimum and maximum TCV positions of 0 and 11. The simulations were run to steady state in the cold and hot thermal environments and

the various temperatures recorded. In some of these simulations, thermal comfort was not maintained.

Table 6 compares the operating ranges determined with EMU experimental and flight data [IT95,Tyl96]. The predicted variable ranges compare well with the experimental data with the exception of the valve module temperature. The valve module temperature predicted by SINDA EMU is on average 18°F (10°C) below the valve module temperature from experimental data and this range is therefore not accurate. The predicted range for the inlet LCG temperature contains the experimental and flight data ranges. The smaller ranges for the experimental and flight data are due to the experimental and flight EVAs not approaching the system's performance boundaries for high metabolic rates and high TCV positions.

4.3 Response Times - The response times of the Shuttle EMU to a change in TCV position indicate how quickly the EMU can restore thermal comfort for the astronaut. The response times (time to 36.8% of steady state value) are calculated for the two variables of interest, $T_{in,lcg}$ and T_{vm}, and recorded in Table 7. For the first four simulations, the metabolic rate was 751 BTU/hr (220 W) for the entire four hours and the TCV position was changed from 0 to 11, 11 to 0, 0 to 7, and 7 to 11 after two hours. The remaining ten simulations in Table 7 were conducted to determine the effect of metabolic rate and environmental temperature on the response times of the EMU variables. For these simulations, different environmental sink temperatures and metabolic rates were prescribed with TCV position changes occurring after two hours.

TCV position changes had little effect on the VG inlet temperatures and dew points. The response times of the inlet LCG temperature and the valve module temperature can be understood by looking at Figure 11 which shows the mass flow rate, as a function of TCV position, through the sublimator portion of the WCL . The slope of the flow rate curve is small up to a TCV position of 7 and then increases significantly for TCV positions 7 to 11. This explains why the inlet LCG and valve module temperatures respond much faster for a TCV change of 0 to 11 than for a TCV change from 0 to 7. The slowest response of the first four cases

16

in Table 7 is the case where there is a TCV change of 11 to 0. The response times for this case are much longer than for the 0 to 11 case. This illustrates the "cold soaked" condition, which has been reported by astronauts frequently. The PLSS thermal mass becomes cold at the high TCV position and it takes a significantly longer time for the astronaut's metabolic heat to warm the system than it does for the sublimator to cool the system down. The response time of the EMU is significantly less when providing cooler water than when providing warmer water to the astronaut. The metabolic rate of the astronaut and environmental temperature have only a small effect on the response times of the EMU variables.

The inlet LCG temperature time constant ranges from 3 to 12 minutes. Therefore, while it may take the EMU as much as 72 minutes to reach steady state and achieve the exact amount of cooling desired, significant cooling or warming can be supplied within a maximum of 12 minutes. The valve module temperature time constant ranges from 9 to 23 minutes. The valve module response times are slower than the LCG inlet temperature since it is only passively cooled by the WCL flowing through it and by thermal interactions with the sublimator and other PLSS components.

4.4 Performance Envelope - The performance envelope of the Shuttle EMU can be seen in Figure 12. This envelope characterizes typical operation of the Shuttle EMU. The Shuttle EMU can operate outside this envelope for short durations, but thermal comfort is difficult or impossible to maintain. The environmental sink temperature and metabolic rate ranges include the typical operations of the EMU as discussed in previous sections. The TCU is not worn in hot environments and high metabolic rates. The duration of the EVA is limited by the feedwater supply and cooling capacity for high metabolic rates.

5.0 CONCLUSIONS

An overview of the thermal dynamic problem for a typical space suit system is provided, with the focus on astronaut thermal comfort control. The SINDA EMU model has been used to analyze the thermal dynamics of the suit with observations verified using experimental and flight data. The evaluation of the SINDA EMU model showed that open loop submodel errors are

magnified in a fully integrated closed loop model. The limitations of the SINDA EMU model are discussed and it is seen that relatively large errors exist for human temperature and PLSS structure temperature predictions. The error quantification showed that temperature prediction errors in the WCL, the human, and the valve module could significantly affect the heat balance in the EMU and therefore make the prediction of human thermal comfort difficult or impossible. Analyzing the SINDA EMU model assumptions revealed that WCL transport delays have a significant effect on the transient temperature predictions in the WCL. The SINDA EMU model was enhanced to include the LCG transport delay, which improved the WCL transient response.

The error quantification demonstrated the difficulty in developing an accurate model of the human-space suit system. With the differences between individuals and between individuals on different days, a high level of accuracy in the human thermal model is difficult unless a model is individualized and correlated with extensive experimentation. Even with the prediction errors seen in the SINDA EMU model, the overall dynamics and interactions of the space suit system are represented. This allows the initial engineering analysis to be conducted and design decisions to be made free from the large expense of experiments.

The performance characteristics of the Shuttle EMU are such that astronaut thermal comfort can be maintained in a wide range of environments and metabolic loads. Heat leaks from space were determined and it was seen that they can often be as large as the astronaut's metabolic rate. This requires that a thermal control strategy explicitly or implicitly account for the environmental conditions. The transient characteristics of the Shuttle EMU showed that the response times of the WCL vary depending on what TCV position is chosen. The inlet LCG temperature responds faster when cooler water is desired than when warmer water is desired. This suggests that future space suit designs include active heating, so that the duration of cold discomfort can be minimized. The inclusion of active heating would also help to increase the low metabolic rate and cold environment portions of the space suit operating envelope. The steady state operating envelope, in terms of environment and metabolic rate, for the Space

Shuttle Suit was defined with the understanding that the suit can provide for thermal comfort for short periods of time outside this envelope.

The observations from this study are being utilized in two future design efforts, automatic thermal comfort control design for the present space suit and design of future space suit systems for Space Station, Lunar, and Martian missions. The two advanced space suit designs presently being developed by NASA are the Minimum Consumables Portable Life Support System (MPLSS) Space Suit and the Cryogenic Oxygen Portable Life Support System (CPLSS) Space Suit. Although different than the Shuttle Suit discussed in this paper, many of the observations made here can be applied to the modeling and design efforts related to these advanced space suits. Both designs include a comfort heater to improve warming response time and help with cold discomfort. Both the advanced PLSS designs have a modular structure which reduces the indirect thermal interactions seen between the Shuttle PLSS components through the valve module. The advanced space suit designs will integrate automatic thermal comfort control into the original design. The advanced space suit system and controller designs are presently underway [Law98].

ACKNOWLEDGMENTS

REFERENCES

[Bue89]   Bue, G.C.   1989.   *Computer Program Documentation 41-Node Transient Metabolic Man Program.* Houston: National Aeronautics and Space Administration, Johnson Space Center. CTSD-0425.

[Cam96]   Campbell, A.B., S.S. Nair, J.B. Miles, and E.W. Webbon. 1996. PLSS Transient Thermal Modeling for Control. *Transactions of the Society of Automotive Engineers, Journal of Aerospace* 105(1): ... SAE 961482.

[Cam97]   Campbell, A.B., S.S. Nair, J.B. Miles, J.V. Iovine, and C.H. Lin. 1997. PLSS Thermal Model Requirements for Control. *Transactions of the Society of Automotive Engineers, Journal of Aerospace* 106(1): 1062-1072. SAE 972506.

[Cam98]   Campbell, A.B., D.C. Mays, S.S. Nair, J.B. Miles, J.V. Iovine, and C.H. Lin. 1998. EMU Thermal Performance Characteristics. In *28th International Conference on Environmental Systems, held in Danvers, Massachusetts, July 13-16, 1998*. SAE 981720.

[Fre97]   French, J.D., A.D. Viswanath, S.S. Nair, J.B. Miles, and C. Lin. 1997. Evaluation of Parameters and Assumptions of Human Thermal Models for EVA Applications. *Transactions of the Society of Automotive Engineers, Journal of Aerospace* 106(1): 579-586. SAE 972320.

[Ham92]   *Space Shuttle Extravehicular Mobility Unit: Space Suit Assembly (SSA) Mini-Data Book, Life Support Sub-System (LSS) Mini-Data Book*. October 1, 1992. Hamilton Standard Division United Technologies Corporation. Windsor Locks, Connecticut.

[IL96]   Iovine, J.V., Langston, N.L. November 1996. *EMU SINDA Model Verification Upgrades Report*. Houston: Lockheed Martin Engineering & Science Services. LMES-32332.

[IT95]   Iovine, J.V., D.P. Tylutki. November 1995. Memo: STS-69 EMU Post Flight Thermal Analysis. Houston: Lockheed Martin Engineering & Science Services.

[Law98]   Lawson, M., C. Cross, and R. Stinson. 1998. The Advanced Space Suit Project - 97 Update. In *28th International Conference on Environmental Systems, held in Danvers, Massachusetts, July 13-16, 1998*. SAE 981629.

[Lin78]   Lin, C.H. 1978. *Program documentation SINFLO thermal model for simulation of a shuttle extravehicular mobility unit*. Lockheed Electronics Company, Inc. NASA-JSC: JSC-14445.

[Smi93]   Smith, L.F., S.S. Nair, J.B. Miles, and B.W. Webbon. 1993. Evaluating Human Thermal Models for Advanced Portable Life Support System Control Development. *Transactions of the Society of Automotive Engineers, Journal of Aerospace* 102: 1193-1203. SAE 932186.

[Tho94]   Thomas, G. 1994. Shuttle EMU Analytical Model Correlation Study Test Plan Document. Crew Systems Division NASA-JSC: JSC-38081.

[TT97]Thomas, G.A. and L.A. Trevino. 1997. Extravehicular Activity Metabolic Profile Development Based on Apollo, Skylab, and Shuttle Missions. In *27th International Conference on Environmental Systems, held in Lake Tahoe, Nevada, July 14-17, 1997*. SAE 972502.

[Tyl96]   Tylutki, D.P. March 1996. Memo: STS-72 EMU Post Flight Thermal Analysis. Houston: Lockheed Martin Engineering & Science Services.

NOMENCLATURE

CCC: Contaminant Control Cartridge

DCM:	Display and Controls Module
EMU:	Extravehicular Mobility Unit
EVA:	Extravehicular Activity
F/P/S:	Fan/Pump/Separator
HUT:	Hard Upper Torso
LCG:	Liquid Cooling Garment
LCVG:	Liquid Cooling and Ventilation Garment
MR:	Metabolic Rate
PLSS:	Portable Life Support System
Q_{stor}:	Total Body Heat Storage
SINDA:	Systems Improved Numerical Differencing Analyzer
SSA:	Space Suit Assembly
TCU:	Thermal Comfort Undergarment
TCV:	Temperature Control Valve
$T_{in,lcg}$:	LCG Inlet Temperature
$T_{in,vg}$:	VG Inlet Temperature
$T_{in,dew}$:	VG Inlet Dew Point
T_{vm}:	Valve module temperature at HUT interface
TMG:	Thermal Meteoroid Garment
VG:	Ventilation Garment
VL:	Ventilation Loop
WCL:	Water Cooling Loop

TABLES

Table 1: Range of temperature differences (simulation - experiment) for Integrated Model Analysis.

Variable Subject	$T_{in,lcg}$, °F (°C)	$T_{out,lcg}$, °F (°C)	$T_{in,vg}$, °F (°C)	$T_{out,vg}$, °F (°C)
Subject 1	-3 to +3 (-1.7 to +1.7)	-2 to +3 (-1.1 to +1.7)	-3 to 0 (-1.7 to 0)	+3 to +6 (+1.7 to +3.3)
Subject 2	-5 to +5 (-2.8 to +2.8)	-4 to +5 (-2.2 to +2.8)	-3 to +1 (-1.7 to +0.6)	+3 to +10 (+1.7 to +5.6)
Subject 3	-18 to +5 (-10 to +2.8)	-18 to +5 (-10 to +2.8)	-13 to +2 (-7.2 to +1.1)	-4 to +7 (-2.2 to +3.9)

Variable Subject	$T_{in,dew}$, °F (°C)	$T_{out,dew}$, °F (°C)	T_{core}, °F (°C)	T_{skin}, °F (°C)
Subject 1	-3 to +4 (-1.7 to +2.2)	-3 to +11 (-1.7 to +6.1)	-2 to 0 (-1.1 to 0)	+6 to +13 (+3.3 to +7.2)
Subject 2	0 to +6 (0 to +3.3)	-15 to +8 (-8.3 to +4.4)	-1 to +1 (-0.6 to +0.6)	+5 to +15 (+2.8 to +8.3)
Subject 3	-7 to +8 (-3.9 to +4.4)	-8 to +7 (-4.4 to +3.9)	-2 to 0 (-1.1 to 0)	-1 to +9 (-0.6 to +5)

Table 2: Range of temperature differences (simulation - experimental) for PLSS Submodel Analysis.

Variable Subject	$T_{in,lcg}$, °F (°C)	$T_{in,vg}$, °F (°C)	$T_{in,dew}$, °F (°C)
Subject 1	-2 to +1 (-1.1 to +0.6)	-4 to +1 (-2.2 to +0.6)	-4 to +5 (-2.2 to +2.8)
Subject 2	-2 to 0 (-1.1 to 0)	-3 to +1 (-1.7 to +0.6)	-2 to +9 (-1.1 to +5)
Subject 3	-8 to 0 (-4.4 to 0)	-7 to +9 (-3.9 to +5)	-9 to +19 (-5 to +10.6)

Table 3: Comparison of differences between simulated and experimental results.

a) Heat Transfer for WCL and VL.

	ΔT_{error}, °F (°C)	$\dot{Q}_{error}$, BTU/hr (W)	Percent of Average MR
WCL Temperature	± 1 (± 0.6)	± 240 (± 70)	32.0%
VL Temperature	± 5 (± 2.8)	± 10 (± 2.9)	1.3%
VL Dew Point	± 5 (± 2.8)	± 36* (± 11)	4.8%

b) Heat Content.

	ΔT_{error}, °F (°C)	Q_{error}, BTU (W-hr)	Percent of Common Band
Valve Module	± 18 (± 10)	± 36.72 (± 10.8)	56.5%
Skin Temperature	± 5 (± 2.8)	± 35.35 (± 10.4)	54.4%
Core Temperature	± 1 (± 0.6)	± 42.92 (± 12.6)	66.0%

*Varies with VL temperature and dew points

22

Table 4: Space Shuttle EVA environmental sink temperatures and heat leaks to EMU generated with SINDA EMU.

Orbital Environments	Sink Temperature, °F (°C)	Total Heat Leak, BTU/hr (W)	Suit Heat Leak, BTU/hr (W)	PLSS Heat Leak, BTU/hr (W)
Cold	-130 (-90)	-449 to -388 (-132 to -114)	-293 to -247 (-86 to -72)	-156 to -141 (-46 to -41)
Neutral	70 (21.1)	-49 to +35 (-14 to +10)	-35 to +28 (-10 to +8)	-14 to +7 (-4 to +2)
Hot	220 (104)	+781 to +815 (+229 to +239)	+500 to +524 (+147 to +154)	+281 to +291 (+82 to +85)

Table 5: Space Shuttle EMU thermal comfort rating for two-hour EVA simulation in various thermal environments.

Metabolic Rate Sink Temperature, °F (°C)	Comfort Rating, $Q_{stor} - Q_{stor,nom}$, BTU (W-hr)		
	400 BTU/hr (117 W)	751 BTU/hr (220 W)	1276 BTU/hr (374 W)
-130 (-90)	cold, <-190 (<-56)	comfort,+6 (+1.8)	comfort,+1 (+0.3)
70 (21.1)	comfort,+7 (+2.1)	comfort,+3 (+0.9)	hot,+86 (+25)
220 (104)	comfort,+2 (+0.6)	comfort,+1 (+0.3)	hot,>+524 (>+154)

Note: > increasing after 2 hour simulation   < decreasing after 2 hour simulation

Table 6: Comparison of predicted operating ranges for EMU variables with experimental [IL96] and flight data [IT95,Tyl96].

|	$T_{in,lcg}$, °F (°C)		$T_{in,vg}$, °F (°C)		$T_{in,dewpt}$, °F (°C)		T_{vm}, °F (°C)	
	Min.	Max.	Min.	Max.	Min.	Max.	Min.	Max.
Predicted	39 (4)	89 (32)	43 (6)	59 (15)	34 (1)	45 (7)	42 (6)	70 (21)
Experimental	45 (7)	85 (29)	46 (8)	60 (16)	30 (-1)	44 (7)	67 (19)	75 (24)
Flight	45 (7)	80 (27)	na	na	na	na	na	na

Note: na = Temperature not available

Table 7: Response times of LCG inlet water and valve module temperatures for simulations with change in TCV position and/or metabolic rate occurring after 2 hours of simulation.

Sink Temperature, °F	TCV Positions	Metabolic Rate, BTU/hr (W)	$T_{in,lcg}$, min.	T_{vm}, min.
70 (21)	0 -> 11	751 (220)	3.0	11.4
70 (21)	11 -> 0	751 (220)	12.0	22.2
70 (21)	0 -> 7	751 (220)	8.4	18.0
70 (21)	7 -> 11	751 (220)	3.0	11.4
-130 (-90)	0 -> 11	751 (220)	3.0	12.0
-130 (-90)	11 -> 0	751 (220)	11.4	20.4
220 (104)	0 -> 11	751 (220)	3.0	9.0
220 (104)	11 -> 0	751 (220)	11.4	23.4
70 (21)	0 -> 11	1276 (374)	3.0	9.0
70 (21)	11 -> 0	1276 (374)	11.4	23.4
70 (21)	0 -> 11	400 (117)	3.0	11.4
70 (21)	11 -> 0	400 (117)	13.2	22.2

| 70 (21) | 0 -> 11 | 400 -> 1276 (117 -> 374) | 3.0 | 9.0 |
| 70 (21) | 11 -> 0 | 1276 -> 400 (374 -> 117) | 8.4 | 16.2 |

FIGURES
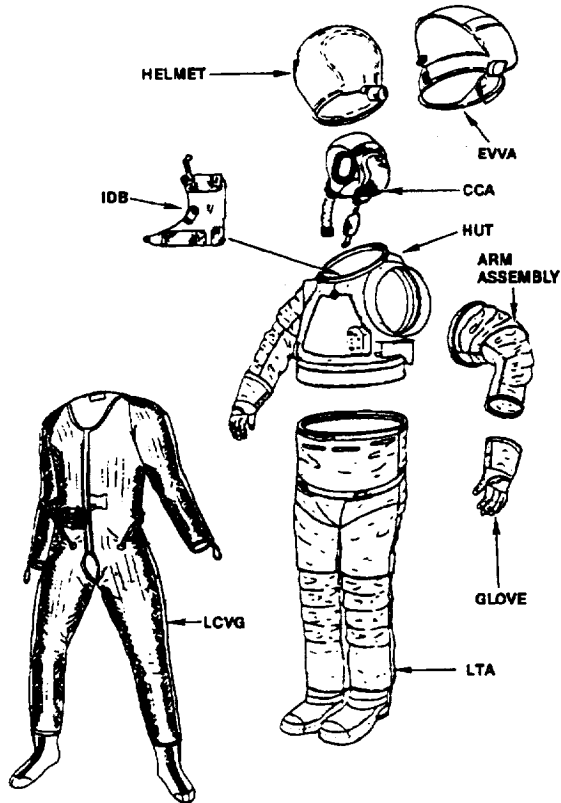
1a)
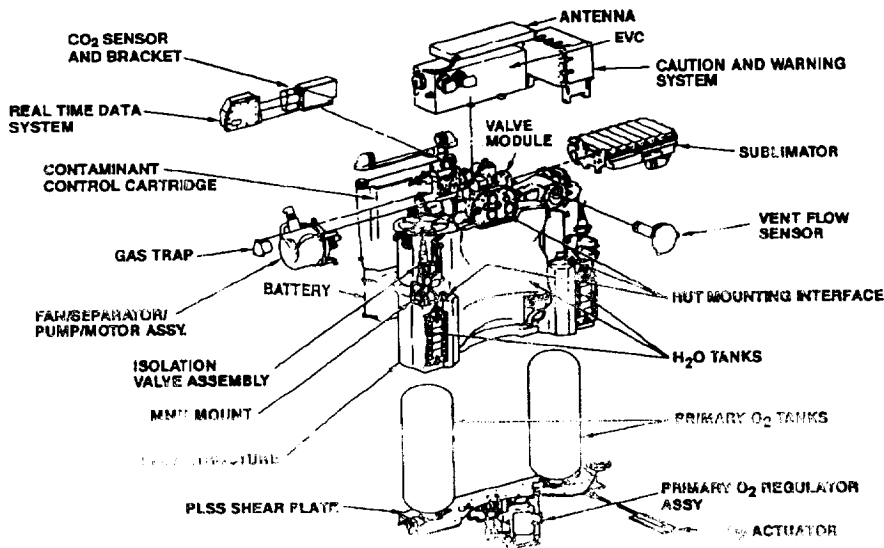
1b)

Figure 1: Space Shuttle EMU [Ham92].

  a. Space Suit Assembly
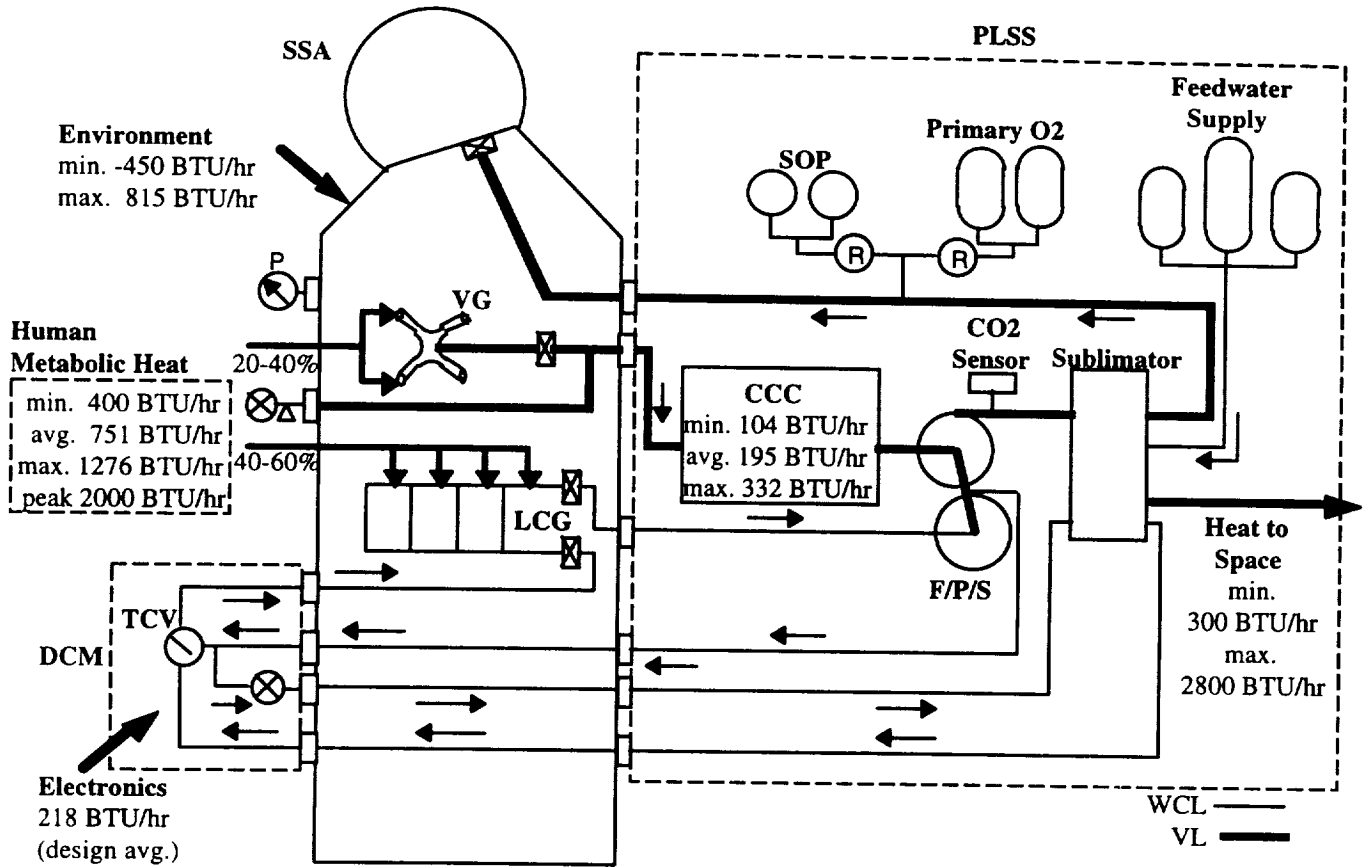 **b.** Portable Life Support System
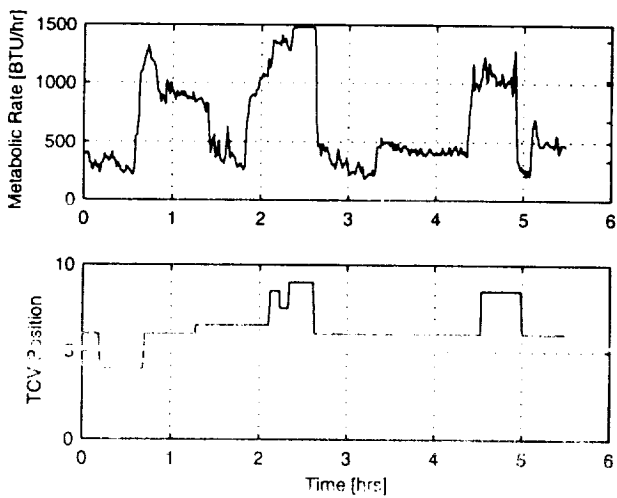
Figure 2: EMU system schematic with heat loads.
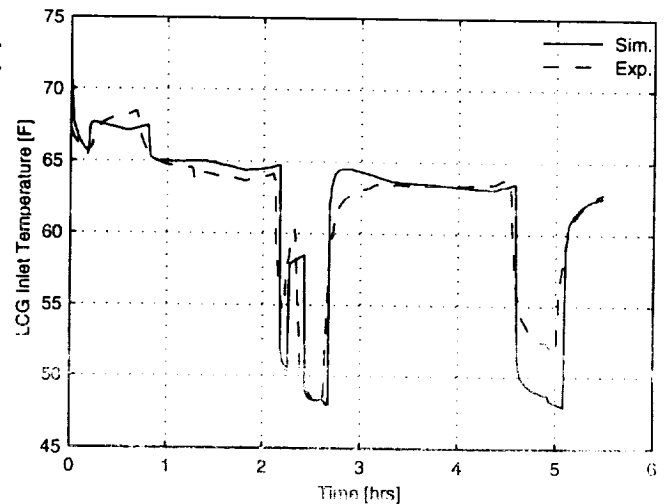

Figure 3: Metabolic rate and TCV positions for Subject 1.

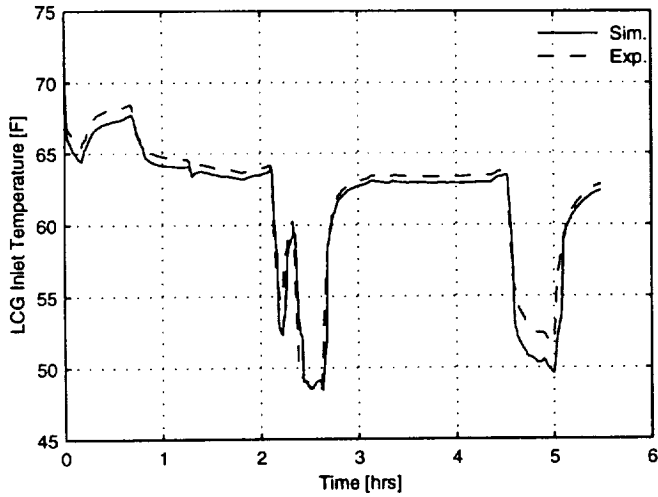Figure 4: Integrated SINDA EMU simulation and experimental LCG inlet temperature for Subject 1.

26

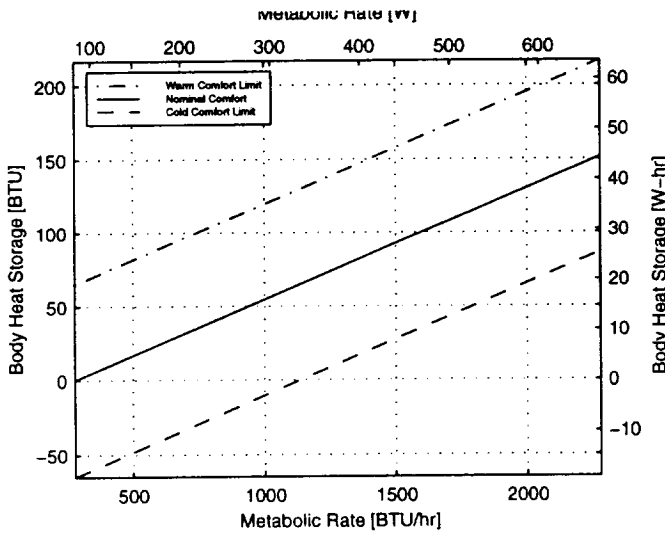**Figure 5:** PLSS Submodel Analysis simulation and experimental LCG inlet temperature for Subject 1.
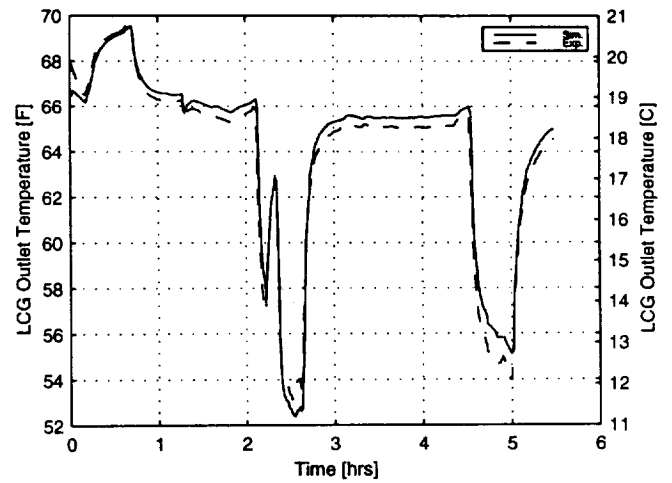
Figure 6: Suit Submodel Analysis simulation and experimental LCG outlet temperature for Subject 1.

Figure 7: Thermal comfort based on total body heat storage and metabolic rate.
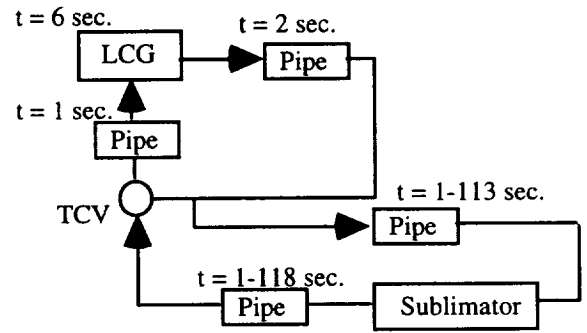

Figure 8: Simplified WCL diagram for transport delay analysis with transport delay range for TCV positions of 11 to 0.
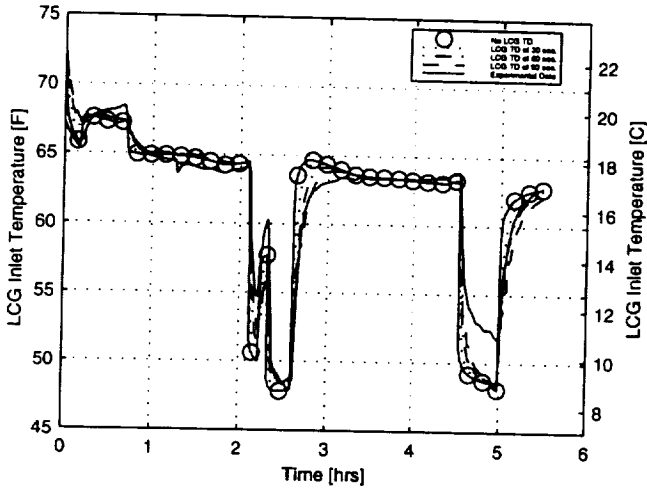
Figure 9: LCG Inlet Water Temperature from SINDA EMU for LCG time delays of approximately 0, 30, 60, and 90 seconds.
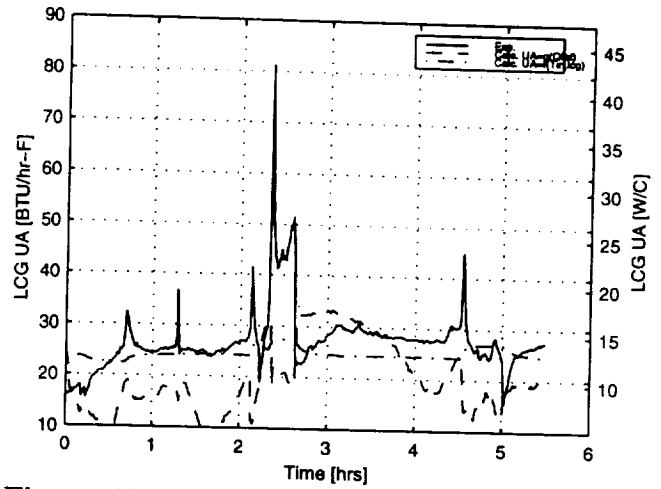

Figure 10: Experimental and Calculated LCG UA for UA=f($T_{in,lcg}$) and UA=g(Q_{lat}).
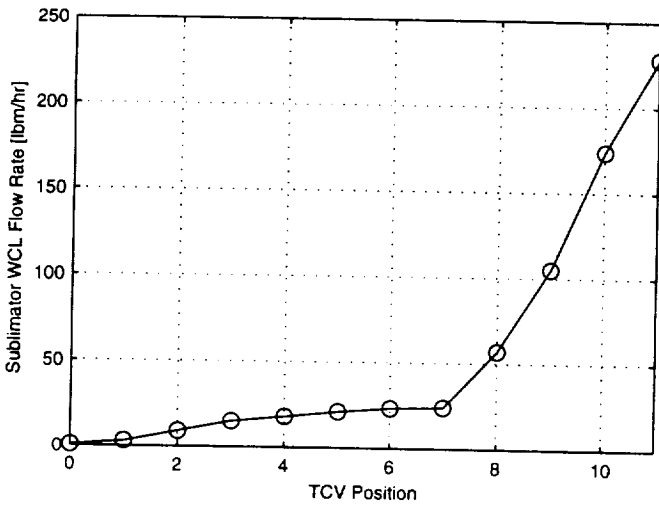

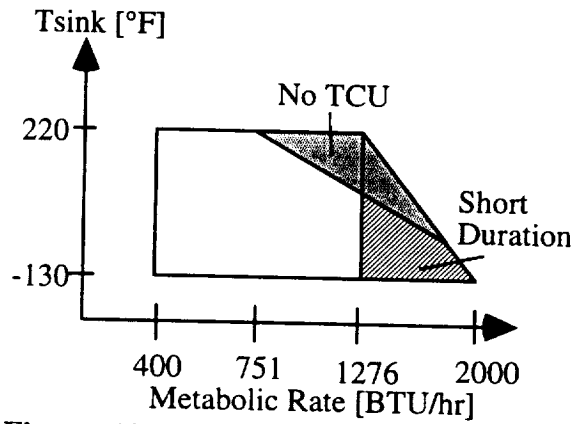**Figure 11:** Sublimator WCL flow rate as a function of TCV position [IL96].

Figure 12: Performance envelope for Shuttle EMU in terms of metabolic rate and environmental sink temperature.

Space Suit Thermal Dynamics

Authors: Anthony B. Campbell, Ph.D. Candidate, Satish S. Nair, Ph.D., John B. Miles, Ph.D., John V. Iovine, and Chin H. Lin, Ph.D.

Motivation:

- To evaluate the Space Shuttle EMU thermal model

- To analyze EMU model assumptions and therefore improve EMU model

- To quantify the sensitivity of the EMU thermal performance to various EMU parameters

- To determine a complete characterization of the EMU thermal performance characteristics and define the limitations of the present Shuttle EMU for providing thermal comfort

- Conclusions can be applied to future EMU designs for Space Station, Lunar, and Mars missions

Contributions:

- Evaluation results for the SINDA EMU model are given and error bands quantified

- EMU operation envelope

- Importance of modeling transport delay quantified and SINDA EMU improved by including the LCG transport delay.

- What did transient analysis show that the SS one did not?
  -response times
  -transport delay
  -thermal comfort

Notes:

*Indicate that new model is being developed
*SI Units with FPS in ()

Summary and Results:
(R=review, P=previous paper summarized, N=new material or extension of previous paper)

1.0 Introduction
        *Describe system and heat loads (R)
        *Give design specifications for EMU (R)
2.0 SINDA EMU Model
        *Describe SINDA EMU Model (R)
        *Describe experimental data (R)
          Experimental Validation
                Integrated Model Analysis
                        *CL System (P, ICES97)
                PLSS Submodel Analysis
                        *OL PLSS (P, ICES97)
                Suit Submodel Analysis
                        *OL Suit (P)
                Validation Conclusions

29

*OL Error magnified in CL system (N)
*List of possible WCL problems (N & P)
*Weakness of 41-Node Man illustrated (N)
*Large errors in valve module temp. cause problems for WCL and VL temp.'s (N)

2.2 Quantifying Errors
*Tin,lcg, Tin,vg, Tin,dew errors converted to heat transfer (P, ICES97)
  Water temperatures most important
*Tskin, Tcore, Tvm errors converted to heat storage (N)
  All three temperature errors significant

3.0 Model Enhancements
3.1 Negligible Thermal Mass
*Valve module and feedwater tanks mass need to be included (P,ICES97)
*WCL and VL masses can be ignored (P)
3.2 Transport Delays
*OL transport delay ranges listed to show significance (P, ICES97)
*Higher TCV setting, the less the transport delay (P)
*Simplified modeling showed that LCG tranport delay is most significant and must be
  included for accurate transient response (N)
*LCG t.d. of 60 sec. chosen to fit experimental data (N)
3.3 LCG Model
*Describe model (R)
Experimental Validation
*Calulate outlet temperature from experimental inputs (N)
*UA did not match experimental in transient sense, but average did (N)
*Conclude that LCG outlet temperature is not sensitive to UA errors (N)
LCG UA Model Comparison
*Compared UA=f(Tin,lcg,mdot) and UA=g(Qlat) (N)
*Conclude that f(Tin,lcg,mdot) is better (N)
LCG Flow Rate
*Compared LCG outlet temp. for flow rates of 240 lbm/hr and 261 lbm/hr (N)
*LCG Outlet temp. not sensitive to small deviations flow rate (N)
LCG Modeling Conclusions
*SINDA EMU errors in LCG outlet water temperature are primarily due to errors in
  Tin,lcg (previous time steps) and Tskin (41-Node man model) (N)
*Focus of future improvements should be on localized modeling (N)
3.4 Valve Module
*Variation of conductance between sublimator plate and valve module (N)
*Conclude that VM temp. significantly effects WCL and VL (N)

4.0 Performance Characteristics and Sizing Issues
4.1 Environment (P,ICES98)
*Varied MR and Tenv (P)
*Defined heat leak ranges and comfort in each extreme situation (P)
4.2 Operating Ranges (P,ICES98)
*Extreme operating ranges defined for key EMU variables and compared with
  experiments and EVA (P)
4.3 Response Times (P,ICES98)
*Determined response times of Tin,lcg and Tvm (P)
*Slower when warming than when cooling (P)
*Recommend next space suit include active heating (P & N)
4.4 Performance Envelope
*Defined operating envelope based on MR, Tenv., TCU, and time (N)
5.0 Summary and Conclusions

BULLET CONCLUSIONS BY INTRODUCTION TOPIC

(i) evaluates the NASA thermal model of the Shuttle EMU

    *OL Error magnified in CL system (N)

    *List of possible WCL problems (N & P)

    *Weakness of 41-Node Man illustrated (N)

    *Large errors in valve module temp. cause problems for WCL and VL temp.'s (N)

(ii) quantifies model prediction errors in terms of heat transfer and heat content errors

    *Tin,lcg, Tin,vg, Tin,dew errors converted to heat transfer (P, ICES97)

        Water temperatures most important

    *Tskin, Tcore, Tvm errors converted to heat storage (N)

        All three temperature errors significant

(iii) defines the limitations of the Shuttle EMU model

(iv) analyzes some of the basic modeling assumptions and determines enhancements to the Shuttle EMU model

    Negligible Thermal Mass

    *Valve module and feedwater tanks mass need to be included (P,ICES97)

    *WCL and VL masses can be ignored (P)

    Transport Delays

    *OL transport delay ranges listed to show significance (P, ICES97)

    *Higher TCV setting, the less the transport delay (P)

    *Simplified modeling showed that LCG tranport delay is most significant and must be included for accurate transient response (N)

    *LCG t.d. of 60 sec. chosen to fit experimental data (N)

    LCG Model

    *Conclude that LCG outlet temperature is not sensitive to UA errors (N)

    *Compared UA=f(Tin,lcg,mdot) & UA=g(Qlat) (N), Conclude that f(Tin,lcg,mdot) is better (N)

    *LCG Outlet temp. not sensitive to small deviations flow rate (N)

    *SINDA EMU errors in LCG outlet water temperature are primarily due to errors in Tin,lcg (previous time steps) and Tskin (41-Node man model) (N)

    *Focus of future improvements should be on localized modeling (N)

    Valve Module

    *Variation of conductance between sublimator plate and valve module (N)

    *Conclude that VM temp. significantly effects WCL and VL (N)

(v) performs simulations using three metabolic rates and three environments (both spanning typical ranges) to determine the associated environmental heat leaks and to check whether thermal comfort is maintained

    *Varied MR and Tenv (P)

    *Defined heat leak ranges and comfort in each extreme situation (P)

(vi) studies four EMU variables representative of the overall thermal state of the human-EMU system in terms of their operating ranges and response times

    *Extreme operating ranges defined for key EMU variables and compared with experiments and EVA (P)

    *Determined response times of Tin,lcg and Tvm (P)

    *Slower when warming than when cooling (P)

    *Recommend next space suit include active heating (P & N)

(vii) defines the performance envelope for the EMU in terms of metabolic rate and environment

    *Defined operating envelope based on MR, Tenv., TCU, and time (N)

31